Check for updates

H2Open Journal

IWA PUBLISHING

© 2023 The Authors

H2Open Journal Vol 6 No 3, 373 doi: 10.2166/h2oj.2023.057

Evaluation of GLDAS soil moisture product over Kermanshah province, Iran

Ata Amini [a,*], Mehdi Karami Moghadam[b], Abdolnabi Abdeh Kolahchi[c], Mehrdad Raheli-Namin[d] and Kaywan Othman Ahmed[e]

[a] Kurdistan Agricultural and Natural Resources Research and Education Center, AREEO, Sanandaj 66169-49688, Iran
[b] Department of Agriculture, Payame Noor University (PNU), Tehran, Iran
[c] Soil Conservation and Watershed Management Research Institute, SCWMRI, AREEO, Tehran 13445-1136, Iran
[d] Science and Research Branch, Islamic Azad University, Ponak, Tehran 5651835979, Iran
[e] Department of Civil Engineering, Faculty of Engineering, Tishk International University, Sulaimani, Iraq
*Corresponding author. E-mail: a.amini@areeo.ac.ir; ata_amini@yahoo.com

AA, 0000-0001-9358-185X

ABSTRACT

Land surface modelling and data assimilation are advanced techniques for generating optimal fields of land surface states and fluxes. In this study, the Global Land Data Assimilation System (GLDAS) data were utilized to investigate the soil moisture variations and droughts in Kermanshah province, northwest Iran. The GLDAS soil moisture data were employed in various depths and compared with observed monthly soil moisture. The monthly and annual moisture data were processed in the Geographic Information System (GIS) environment. To compute the Standardized Precipitation Index, SPI, precipitation data from 2000 to 2014 were used, and the relationship between drought and soil moisture variation was studied. The moisture data from GLDAS had a significant correlation with the most severe wet and dry seasons. The minimum and maximum values of the SPI were determined as −2.077 and 0.931 in 2004 and 2009, respectively, which corresponded to the highest and lowest normalized soil moisture of −1.93 and 1.41. The results showed that GLDAS data can be used to reconstruct spatial and temporal moisture data series.

Key words: drought, GLDAS, precipitation, soil moisture, SPI

HIGHLIGHTS

- Aimed to explore GLDAS data's potential for soil moisture determination.
- Recorded data were compared with GLDAS estimated soil moisture to verify accuracy.
- Examined soil moisture and its link with drought.
- GLDAS data's potential for estimating soil moisture was explored, with implications for drought monitoring and mitigation.
- Focused on drought-prone Kermanshah, needing efficient soil moisture monitoring and management.

INTRODUCTION

Evaluation of temporal and spatial variation of soil moisture may lead to the understanding of eco-hydrological processes (Zuo *et al.* 2019). In watershed management practices, it is of great importance to estimate the soil moisture, especially when studying the soil moisture distribution under vegetation, micro-topography, and precipitation events impacts (Das & Paul 2015). The soil moisture can be estimated using remote sensing, physical modelling, and *in situ* measurements or using a synthetic approach inclusive of such methods (Zeng *et al.* 2016; Zhuang *et al.* 2020). Remote sensing satellites like SMAP (Soil Moisture Active–Passive) have enabled global-scale observations of soil moisture data (Yuan & Quiring 2017). The accuracy of satellite-based data differs both in terms of the data type and the geographical location (Fang *et al.* 2016).

Weather stations are usually non-uniformly distributed over the basins and that is a challenge for accurately studying the spatial variation of parameters (Amini *et al.* 2019a, 2019b). Therefore, researchers in recent decades have used remote sensing and network data to evaluate parameters like soil moisture (Das *et al.* 2008). Using the soil moisture data recorded in 200 stations, Albergel *et al.* (2012) evaluated the extracted data from satellites with ground-based data and models. The results indicated that the satellite-driven soil moisture data simulated by the European Centre for Medium-Range Weather Forecasts' global model (ECMWF) have acceptable accuracy.

This is an Open Access article distributed under the terms of the Creative Commons Attribution Licence (CC BY 4.0), which permits copying, adaptation and redistribution, provided the original work is properly cited (http://creativecommons.org/licenses/by/4.0/).

Downloaded from http://iwaponline.com/h2open/article-pdf/6/3/373/1255552/h2oj0060373.pdf
by guest

One of the drawbacks of *in situ* observation data is that the recording of this data in many areas is done by ground stations with a long-distance and non-uniform distribution. Satellites are a commonly used device for monitoring soil moisture. However, their single satellite period is limited, which may not be sufficient for climate change research (Wagner *et al.* 2012; Zhuang *et al.* 2020). Remote sensing can detect large-scale coverage, but it is highly reliant on the algorithm inversion method (Alizamir *et al.* 2021). Moreover, it cannot measure moisture in deep soil (Zhang *et al.* 2005). Therefore, the research is challenging due to the limitations of current measurements and monitoring techniques. For many applications in the literature, the Global Land Data Assimilation System (GLDAS) soil moisture is considered the reference source of soil moisture. GLDAS data at several spatial scales have been utilized to authorize soil moisture satellite-derived besides *in situ* measurements of soil moisture. That is because it evaluates soil moisture using some models of land surface through model-derived data, satellite observations, and data assimilation *in situ* (Wagner *et al.* 2003; 2012; Li *et al.* 2015; Kim & Choi 2015).

Chen *et al.* (2013) evaluated the moisture of soil precision data found by the Advanced Microwave Scanning Radiometer-Earth Observing System (AMSR-E) as well as the simulated soil moisture through GLDAS versus the observed data for the centre region of Tibet. According to the results, no output of AMSR-E has a good enough estimation of soil moisture in cold seasons of the year. It was found that the data obtained by the GLDAS model regarding the simulated soil moisture underestimated the soil moisture at the surface (0–5 cm). However, for a layer of 20–40 cm from the ground surface, the amount of moisture was evaluated with appropriate accuracy. Velde *et al.* (2014) presented the soil moisture map by using a microwave sensor for the Tibetan Plateau and validated the results to estimate soil moisture using GLDAS data which pointed out the sensor's capability. By the usage of an assimilation algorithm, Xiao *et al.* (2016) completed the soil moisture data of the satellite spatially and temporally during a 1-year period. The results illustrated that the data from the assimilation algorithm can effectively restore the time series of soil moisture both spatially and temporally in agreement with the simulated data given by the GLDAS model. Yuan & Quiring (2017) evaluated the data of soil moisture simulated and Coupled Model Intercomparison models, CMIP5 for the United States using the station and satellite data. They showed that the CMIP5 models overestimated the usefulness of the near-surface soil moisture (0–10 cm) and the soil column moisture (0–100 cm) in the western and underestimated them in the eastern parts of the US. Using GLDAS data, Park *et al.* (2017) suggested a soil moisture downscaling model. A time series pattern was visible in the 1 km moisture in the soil downscaled similar to that of GLDAS and weather stations.

Drought is usually viewed as one of the costliest natural hazards over the globe, causing damaging impacts on society and eco-environment (Shen *et al.* 2022). Liu *et al.* (2019) compared the two datasets GLDAS surface soil moisture and multi-satellite retrieved data for global drought analysis. According to the results, both datasets exemplify analogous patterns of duration, frequency, and severity of the drought. Drought indices including the Standardized Precipitation Index (SPI) have been widely used in the analysis and monitoring of drought events (Um *et al.* 2018). A methodology using the SPI was proposed by Aksoy *et al.* (2021) to develop critical drought intensity-duration-frequency (IDF) curves. Sun *et al.* (2022) proposed a Modified Drought Severity Index (MDSI) with a local optimization method. They evaluated the drought monitoring performance of MDSI across China and detected high correlations between MDSI and soil moisture, SPI at a 3-month scale, and Actual Drought-Affected Areas (ADA).

GLDAS assessment is usually limited to observation-rich regions of the world. However, only a few assessment activities have been conducted in the Middle East (Bi *et al.* 2016), particularly in a semiarid area such as northwest Iran which encountered several environmental perils (Amini 2020). Knowledge of spatio-temporal variation of soil moisture particularly in the no-station areas is conducive to recognition and prediction of the hazards. To use these databases properly, a consideration of their accuracy and efficiency is required. The aim of this research was to investigate the possibility of using the GLDAS data in determining soil moisture over Kermanshah province, Iran. Also, an investigation of soil moisture was conducted and its relationship with drought was explored. For this purpose, measured data related to GLDAS data at different soil depths during the period 2000–2014 were used. Statistical indicators were used to evaluate GLDAS data, and the relationship between soil moisture and drought was obtained.

Downloaded from http://iwaponline.com/h2open/article-pdf/6/3/373/1255552/h2oj0060373.pdf
by guest

RESEARCH METHOD

The study site

Kermanshah province is located in the west of Iran with a height of 1,332 m between the latitudes of 33° 36′ N to 35° 15′ N, and longitudes 45° 24′ E to 48° 30′ E. The annual average precipitation of the province is 430 mm and the total annual precipitation in the province is around 11 billion cubic meters. The Ravansar station enjoys maximum average precipitation of 530 mm, while the minimum belongs to the Qasr-e-Shirin station with an average of 360 mm. The water resources of the study area include surface and groundwater. In all stations, the season with no rainfall or with very little rainfall begins in May and continues to September. The utmost rainfall event is recorded in February and the lowest corresponds to August. The monthly distribution of rainfall in this region indicates the predominance of winter rainfall. The location of the 13 synoptic stations in the site study and networked points of GLDAS are shown in Figure 1. The stations established in the northern areas undergo the humid Mediterranean climate, and those located west, east, and centre of the province enjoy the semiarid climate.

Soil features

The soil of the study area evolved under the influence of climate and other environmental factors having been engaged in the transport of calcareous materials and their compaction within different soil classes. Due to the area expansion, the soil typification map was provided based on FAO classification (FAO 2015), and then it was digitalized by the GIS to overlap with other information layers. The soil classes studied based on FAO classification are shown in Figure 2. The scope of the current study includes eight main FAO soil classes.

GLDAS

The GLDAS model was developed to generate optimal fields of land surface states. It does so by combining satellite-based and ground data products based on observation and employing data adaptation algorithms and modelling of land surface to keep track of the changes (Rodell *et al.* 2004). The model was cooperatively devised by the scientists of the National Centre for Environmental Prediction (NCEP), the National Oceanic and Atmospheric Administration (NOAA), the Goddard Space Flight Centre, and the National Aeronautics and Space

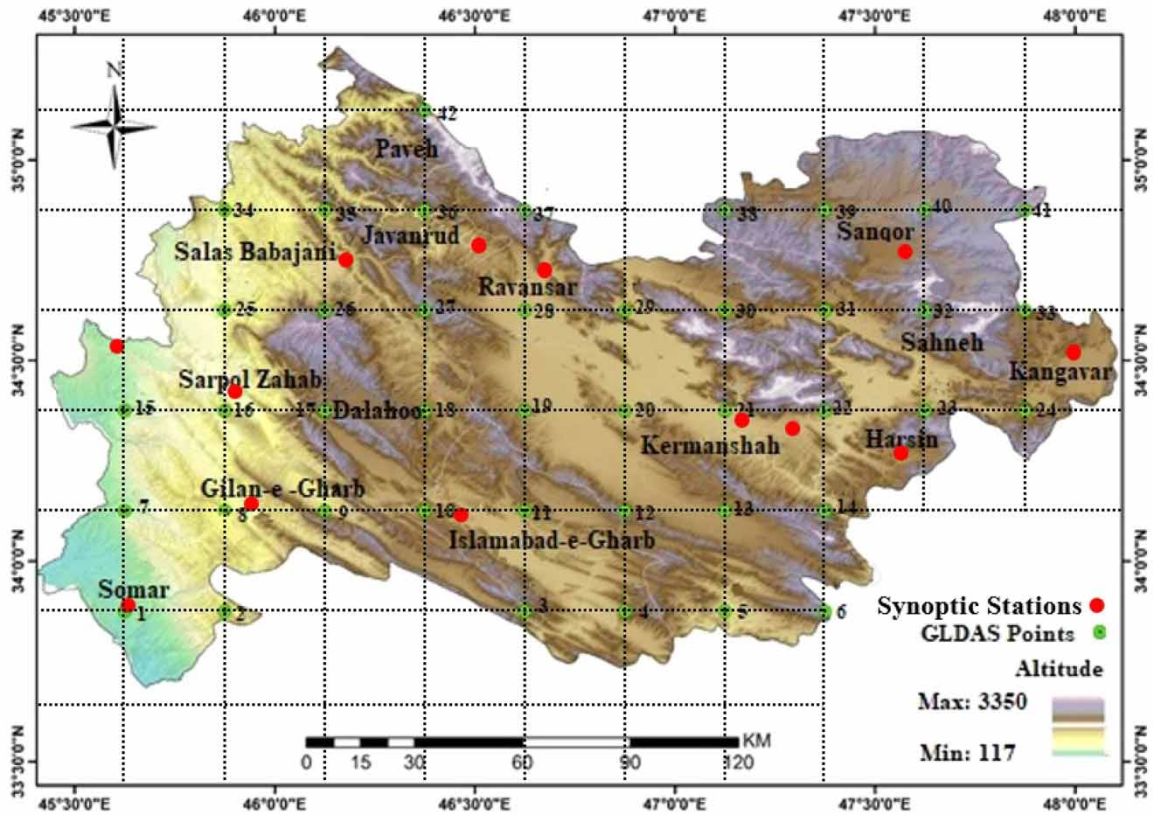

Figure 1 | Geographical location of synoptic stations and networked points of GLDAS in Kermanshah province.

Downloaded from http://iwaponline.com/h2open/article-pdf/6/3/373/1255552/h2oj0060373.pdf
by guest

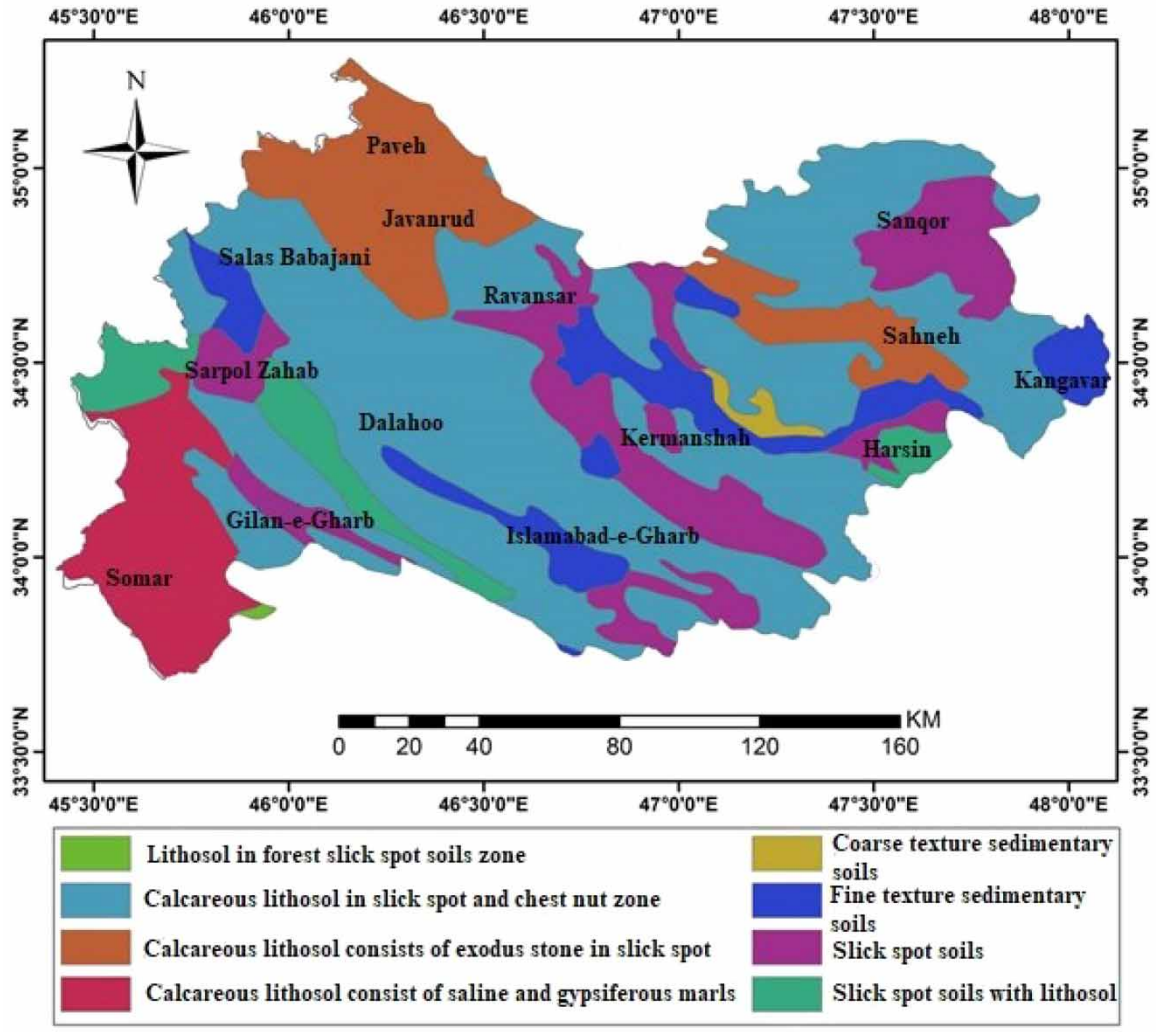

Figure 2 | Soil classes of Kermanshah province on the basis of FAO classification (FAO 2015).

Administration (NASA) to generate various products. It provides users with a collection of land surface water and energy fluxes including moisture data of the soil in four depths of 0–10, 10–40, 40–100, and 100–200 cm (Cai *et al.* 2017). To generate optimal fields of land surface states and fluxes, the GLDAS integrates ground-based data and satellite sets to parameterize, force, and constrain a set of offline land surface models. The Goddard Earth Sciences Data and Information Services Centre website hosts and distributes the GLDAS data. The GLDAS model generates and integrates several global and observation-based data at multi-resolutions. The overall GLDAS modelling strategy is offline land surface models, to integrate multiple, large amounts of observational data and be activated globally by the Land Information System. The resolution of GLDAS products is 3 h. In addition, through the average temporal of 3-h products, the monthly products are produced (Bi *et al.* 2016).

Model verification

In this research, the accuracy of GLDAS data was evaluated by statistical indicators such as coefficients of determination, R^2, agreement coefficient, IA, Root Mean Square Error (RMSE), bias in the MATLAB software environment, and unbiased RMSE, ubRMSE. The R^2 coefficient was calculated from the Equation (1) (Yan *et al.* 2014):

$$R^2 = \frac{\left[\sum_{i=1}^{n}(P_i - \overline{P})(O_i - \overline{O})\right]^2}{\sum_{i=1}^{n}(P_i - \overline{P})^2 \sum_{i=1}^{n}(O_i - \overline{O})^2} \quad (1)$$

Downloaded from http://iwaponline.com/h2open/article-pdf/6/3/373/1255552/h2oj0060373.pdf
by guest

Equation (2) yielded the coefficient IA, which is the rate of sign agreement among the two time series values (Ji & Gallo 2006):

$$IA = 1 - \frac{\sum_{i=1}^{n} (P_i - O_i)^2}{\sum_{i=1}^{n} \left(|P_i - \overline{P}| + |O_i - \overline{O}|\right)^2} \tag{2}$$

Through the following equation, the RMSE was computed:

$$\text{RMSE} = \sqrt{\frac{1}{n}\sum_{i=1}^{i=n} (P_i - O_i)^2} \tag{3}$$

The coefficient bias determines the differences between the observed and the model's data, and is given by Equation (4) (Ouatiki *et al.* 2017):

$$\text{Bias} = \frac{1}{n}\sum_{i=1}^{n} (P_i - O_i) \tag{4}$$

The bias may be easily removed in order to produce a more reliable calculation of RMSE by defining random error characterizing ubRMSE. Equation (5) is used to determine the ubRMSE:

$$ubRMSE = \sqrt{RMSE^2 - Bias^2} \tag{5}$$

where n, P_i, O_i, $\overline{P}$, $\overline{O}$, R, σ_P, σ_O are, respectively, the data number, the value of soil moisture in GLDAS model, the observed value of moisture in the soil, the average moisture of soil in the GLDAS model, the average observational soil moisture, the relationship coefficient among the observational and the moisture model, the model's data standard deviation, and the standard deviation of the observational data.

Drought index

In this investigation to monitor the drought, we used the SPI for the annual timescale. The dimensionless index, SPI, whose positive values indicate wet, and the negative values of which signal drought. The values of this index run below or equal to −2 for extremely dry conditions, and range from +2 and beyond for extreme wet situations. The SPI, which is a precipitation translation into a drought index, was calculated through Equation (6) (Fatemi & Narangifard 2018):

$$SPI = \frac{P_i - \overline{P}}{\sigma} \tag{6}$$

In Equation (6), P_i, $\overline{P}$, and σ stand for the ith year precipitation, the average precipitation, and the standard deviation, respectively.

Data analysis

At meteorological stations, soil moisture is recorded at various depths of 5, 10, 20, 30, 50, 70, 100, 150, and 200 cm and at weekly, daily, and hourly time scales. The moisture in the soil was measured using Time Domain Reflectometry (TDR) equipment. For conductivity of electrical and soil water content measuring, the TDR is a well-known and accurate method (Skierucha *et al.* 2012). In this research, the measured data corresponding to the GLDAS data was used. The data of moisture in the soil pertaining to the synoptic stations of the study area and the networked data related to the GLDAS model with a spatial resolution of 0.25° × 0.25° for depths 0–10, 10–40, 40–100, and 100–200 cm from the ground during the 2000–2014 period were received and processed. Given this resolution, every single point represents the distribution of moisture in the soil throughout the grid with a 25 × 25 km dimension. The analysis of the GLDAS model implied that 42 grids of the model cover the study area. The points which represent each grid of the GLDAS network are designated in Figure 1.

Downloaded from http://iwaponline.com/h2open/article-pdf/6/3/373/1255552/h2oj0060373.pdf
by guest

Data processing was carried out for all these points on a monthly and annual scale in the Geographic Information System (GIS) environment. Afterwards, the monthly soil moisture time series with reference to the different points of the network went into the analysis stage. The Kriging method was used to prepare the soil moisture map. Kriging provides a wide and flexible range of tools that provide estimates for unsampled locations by using a weighted average of neighbouring field values that fall within a certain distance. Kriging allows us to estimate the accuracy of predicting a value given sample values at other locations (Lakhankar *et al.* 2010). Statistical indicators were applied to the GLDAS data for evaluation. Thereby, the soil moisture data associated with the Sararoud station were compared with the data of the nearest point of the GLDAS network in 0–10 cm of the ground, during the years 2006–2012. The evaluations were done through the software environments of MATLAB, SPSS, and MS-Excel. Reviewing of the average soil moisture content during the statistical period as well as annual and monthly monitoring of soil moisture was conducted following the evaluation of GLDAS model data accuracy. Using the data of precipitation in the study area during the statistical period, the drought index of SPI was calculated. Then, the alterations of this index were compared with those of the soil moisture. Figure 3 shows the flowchart that shows the methodology in this research.

RESULTS AND DISCUSSION

Verification of GLDAS

To evaluate the estimations from the GLDAS model versus soil moisture collected from stations, the former was processed for the nearest point to the Sararoud station during the period of 2006–2012 (84 months). The Sararoud station was with the longest and most complete observed data in the area of study. The observed and predicted moisture data in the soil are shown in Table 1. As regards monthly scale and among the cold months of the year, January enjoyed the most surface soil moisture and August experienced the least. The average soil moisture in the Sararoud station occurs at the surface layer of 14.56 kg/m^2.

Figure 4 revealed the monthly comparison of the moisture content in the soil of the Sararoud station and the GLDAS model. As Figure 4 shows, the GLDAS model data have good agreement with soil moisture data.

Table 2 contains the results concerning data accuracy regarding the GLDAS model against the data of the Sararoud station under various statistical indicators.

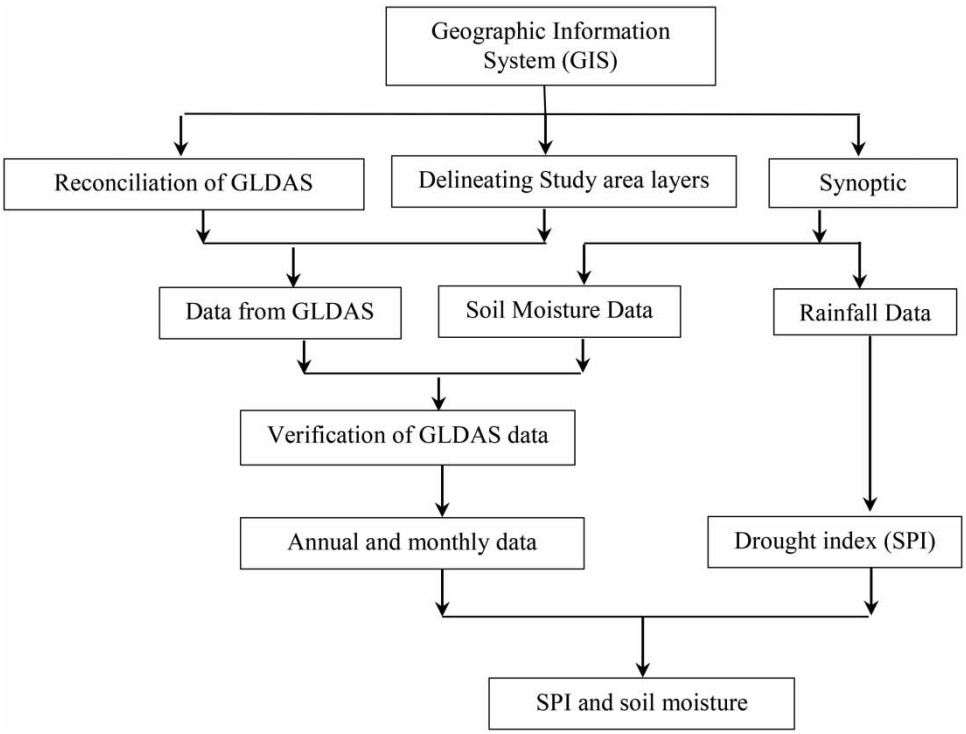

Figure 3 | The research methodology.

Downloaded from http://iwaponline.com/h2open/article-pdf/6/3/373/1255552/h2oj0060373.pdf
by guest

Table 1 | Soil moisture observation and GLDAS data (0–10 cm)

Month/Year	Jan	Feb	Mar	Apr	May	June	July	Aug	Sep	Oct	Nov	Dec
Observed soil moisture (kg/m^2)												
2006	21.87	24.40	20.40	20.63	17.16	9.91	7.57	6.77	7.55	11.60	24.67	22.00
2007	27.67	24.50	22.50	23.33	18.75	6.75	7.68	7.27	6.86	7.08	6.50	12.50
2008	13.50	19.00	16.25	6.25	7.75	8.13	6.92	6.89	9.81	10.13	23.50	20.33
2009	20.33	20.67	27.00	21.00	19.00	8.80	7.19	6.44	9.48	11.26	18.87	18.86
2010	20.27	20.73	19.56	20.05	18.24	10.67	7.20	6.96	8.99	7.69	17.50	9.00
2011	21.00	24.00	18.67	18.80	17.50	5.25	7.31	6.63	6.19	9.94	28.00	22.00
2012	20.75	23.00	24.33	17.50	12.25	3.60	7.67	7.47	6.80	9.68	17.02	17.90
The GLDAS' soil moisture data (kg/m^2)												
2006	27.09	30.16	25.29	25.58	21.36	12.54	9.69	8.71	9.66	14.59	23.21	23.52
2007	39.73	35.62	26.76	27.52	23.20	14.52	9.83	9.32	8.83	9.09	13.09	21.93
2008	28.64	29.84	21.01	17.55	14.05	10.37	8.90	8.86	12.42	12.80	21.24	22.58
2009	26.75	24.75	22.36	23.10	20.19	12.83	9.22	8.32	12.01	14.17	23.43	23.42
2010	25.14	25.70	24.28	24.87	22.67	13.46	9.24	8.95	11.42	9.84	17.25	18.44
2011	21.98	30.21	23.54	21.59	20.77	12.42	9.37	8.55	8.01	12.57	21.49	20.60
2012	19.70	27.43	22.00	24.13	17.79	11.91	9.81	9.57	8.75	12.26	21.18	22.26

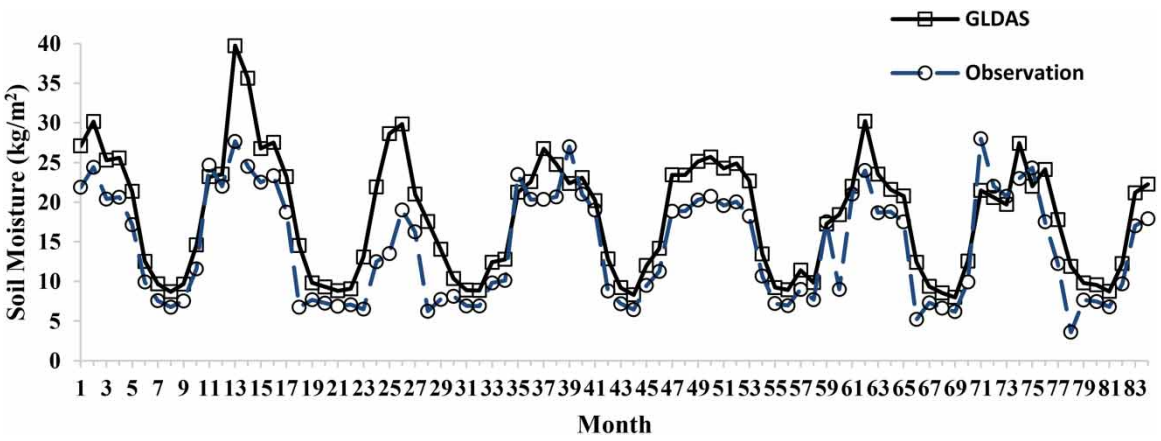

Figure 4 | Comparison of the monthly moisture and the GLDAS model.

Table 2 | Statistical indicators for GLDAS model data and observed data in the Sararoud station (0–10 cm)

Statistical indicators	R^2	IA	RMSE	Bias	ubRMSE
Values	0.79	0.87	4.98	3.63	3.40

The coefficient of determination and agreement index in Table 2 shows relative conformity between the values of the measured moisture of soil and the GLDAS data. The bias index shows an average moisture difference of 3.63 kg/m^2 between the observed and GLDAS data. According to the output of the statistical indicators presented in Table 2, the efficiency of the GLDAS model in the estimation of monthly soil moisture is judged 'good' to 'normal'. These studies show that the model efficiency may vary in different areas. Almost the same labelling for the efficiency of the GLDAS model was due to Velde *et al.* (2014), Xiao *et al.* (2016), and Park *et al.* (2017). Based on the statistical analysis, the GLDAS data could be used as soil moisture representative for the study area.

Downloaded from http://iwaponline.com/h2open/article-pdf/6/3/373/1255552/h2oj0060373.pdf
by guest

Soil moisture

The average values of moisture in the soil during the statistical period, as well as annual and monthly soil moisture were extracted for four different depths as 0–10, 10–40, 40–100, and 100–200 cm from the ground level. The results are shown in Figure 5.

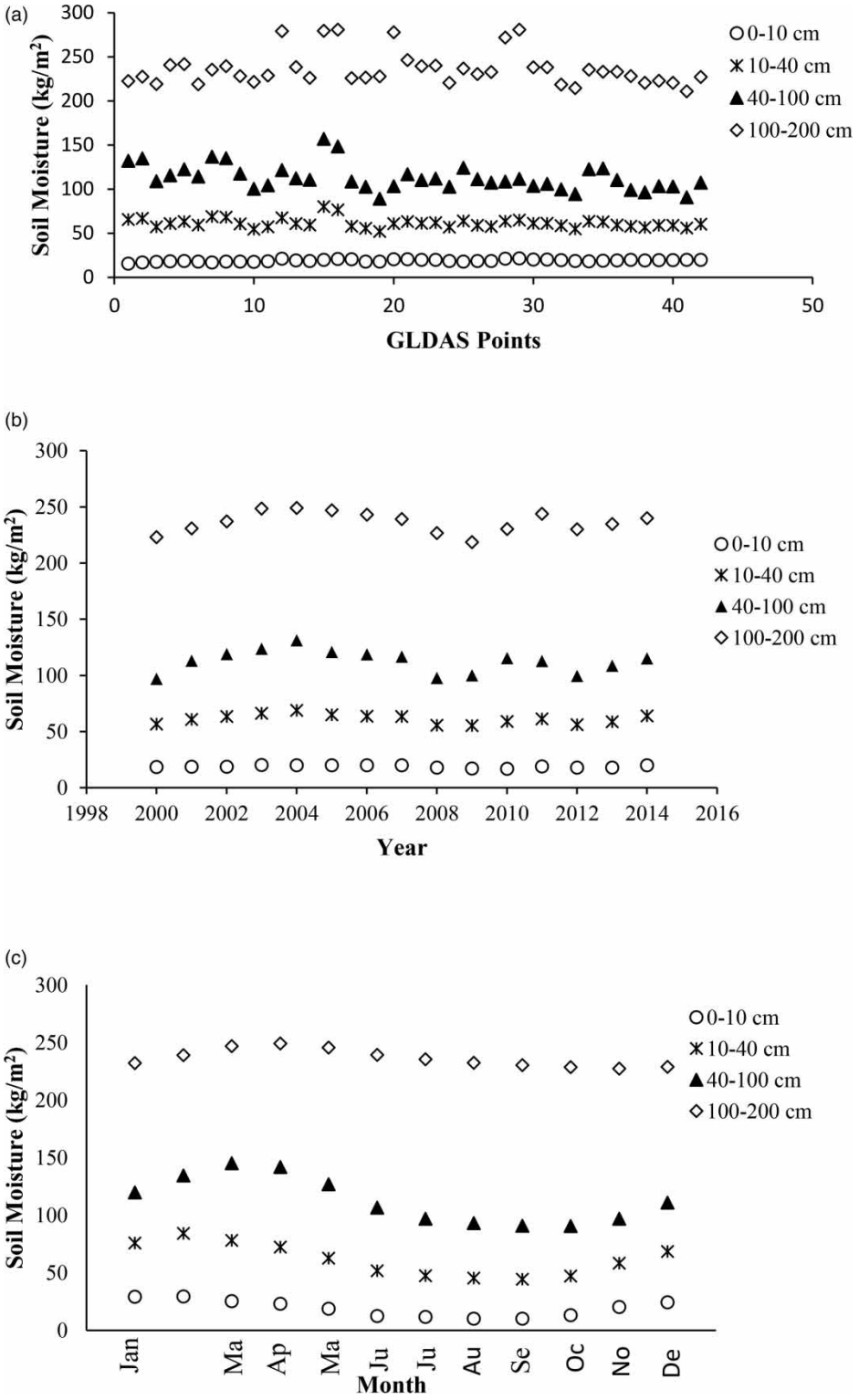

Figure 5 | Soil moisture in the study area obtained from the GLDAS model in different depths: (a) average in 42 points of the GLDAS model; (b) annual average; and (c) monthly average.

Downloaded from http://iwaponline.com/h2open/article-pdf/6/3/373/1255552/h2oj0060373.pdf
by guest

Average moisture

The average values of soil moisture concerning 42 points of the GLDAS model during the statistical period in different depths are shown in Figure 5(a). As seen in Figure 5(a), moisture increases, along with the growth of depth, which agrees with the reported results by Cai *et al.* (2017). The average moisture of soil in the second, third, and fourth layers has been multiplied proportionately to the first layer as 3.2, 6, and 12.5 times, respectively. Incidentally, the average moisture of the fourth layer has increased 2.1 times relative to the third layer.

Annual moisture

The average moisture in the study area for different depths on the annual scale during the 2000–2014 period is shown in Figure 5(b). Figure 5(b) gives the averages in depths 0–10, 10–40, 40–100, and 100–200 cm during the statistical period as 18.92, 61.27, 112.72, and 236.17 kg/m^2, respectively. The variations of annual average surface soil moisture are usually slight and are amplified in parallel with the growth of depth. On the annual scale, the values of moisture in the soil at depths 0–10 cm have not undergone palpable variations; however, from 2007 onward, a decreasing trend has commenced in the surface layer and has been lengthened to 2010. The least value of soil moisture in 2010 is reported to be 16.92 kg/m^2, and the utmost value obtained in 2007 was to be 20.16 kg/m^2. As for the depths 10–40 cm, a rising trend of moisture content in soil in the period 2000–2004 was observed, and a reverse decreasing drift occurred in the years 2004–2009 before a second almost increment trend from 2009 on. With regard to the depths 40–100 cm, one discerns an increasing trend up to the year 2004, and following that, a decreasing sense is observed towards 2009. The same trend holds for the depths 100–200 cm. In the lowest soil depths, the greatest moisture content was recorded in 2004 and the least was evidenced to happen in 2009. According to Amini *et al.* (2019a, 2019b), the most severe wet and drought in Kermanshah province corresponds, respectively, to the years 2004 and 2009, which is inversely proportional to the soil moisture levels at these periods.

Monthly moisture

Figure 5(c) shows the average soil moisture in different depths on the monthly scale during the statistical period.

Figure 5(c) shows that the maximum average value of moisture in the soil at the depths 0–10 and 10–40 cm obtained in February was, respectively, 29.38 and 84.18 kg/m^2. As to the depths 40–100 cm, the maximum value of 145 kg/m^2 was attained in March, and in depths 100–200 cm it was recorded as 249 kg/m^2 in April. Conversely, the minimum value of average moisture in soil recorded in Kermanshah province for the depth 0–10 cm was obtained in August as 10 kg/m^2, for 10–40 cm in September was 44.43 kg/m^2, as for the 40–100 cm depths the minimum was recorded to be 96.61 kg/m^2 in October, and at depths 100–200 cm it was announced as 227 kg/m^2 in November. Therefore, as the depth increases, the alterations of soil moisture in any layer relative to the other happen with a lag of one month, much in agreement with the results of Cai *et al.* (2017). At shallow depths, i.e., in 0–40 cm of the ground, the increasing and decreasing trends keep pace with each other so that in winter it escalates with high values, and then approaching the warm period the decrement trend carries on to the end of summer.

The monthly variations of soil moisture in depths 10–100 cm are great and in deep layers they are low owing to reduced evaporation in the lower layers. Akin to annual variations, the layers of 40–100 cm and 100–200 cm differ drastically in moisture values on the monthly scale.

Soil moisture zoning maps

Zoning maps in Figure 6(a)–6(h) were supplied with the goal of examining the distribution of average and monthly soil moisture variations in different depths based on the GLDAS model data.

Figure 6(a)–6(d) depicts the mapping of average soil moisture in the study area during 2000–2014 resulting from GLDAS data in four different depths. Figure 6(a) illustrates that in the layer of soil 0–10 cm, the utmost value of moisture in the soil is recorded for Kermanshah City, Ravansar, and Sarpol Zahab. The lowest value of 15 kg/m^2 was associated with Somar, the research site south-west. By and large, the southern parts of the province enjoy less soil moisture than the north. Unlike the soil surface layer, the maximum and minimum average moisture for the 10–40 cm layer was recorded, respectively, as 81 kg/m^2 in the western city of Sarpol Zahab and 51 kg/m^2 in Dalahoo and Kangavar, centrally positioned and the province's eastern region. The central areas at 10–40 cm depth, though not relishing the highest soil moisture, remain among those regions with the most moisture in the ranking of areas (Figure 6(b)). The greatest average soil moisture value of 157 kg/m^2 in 40–100 cm

Downloaded from http://iwaponline.com/h2open/article-pdf/6/3/373/1255552/h2oj0060373.pdf
by guest

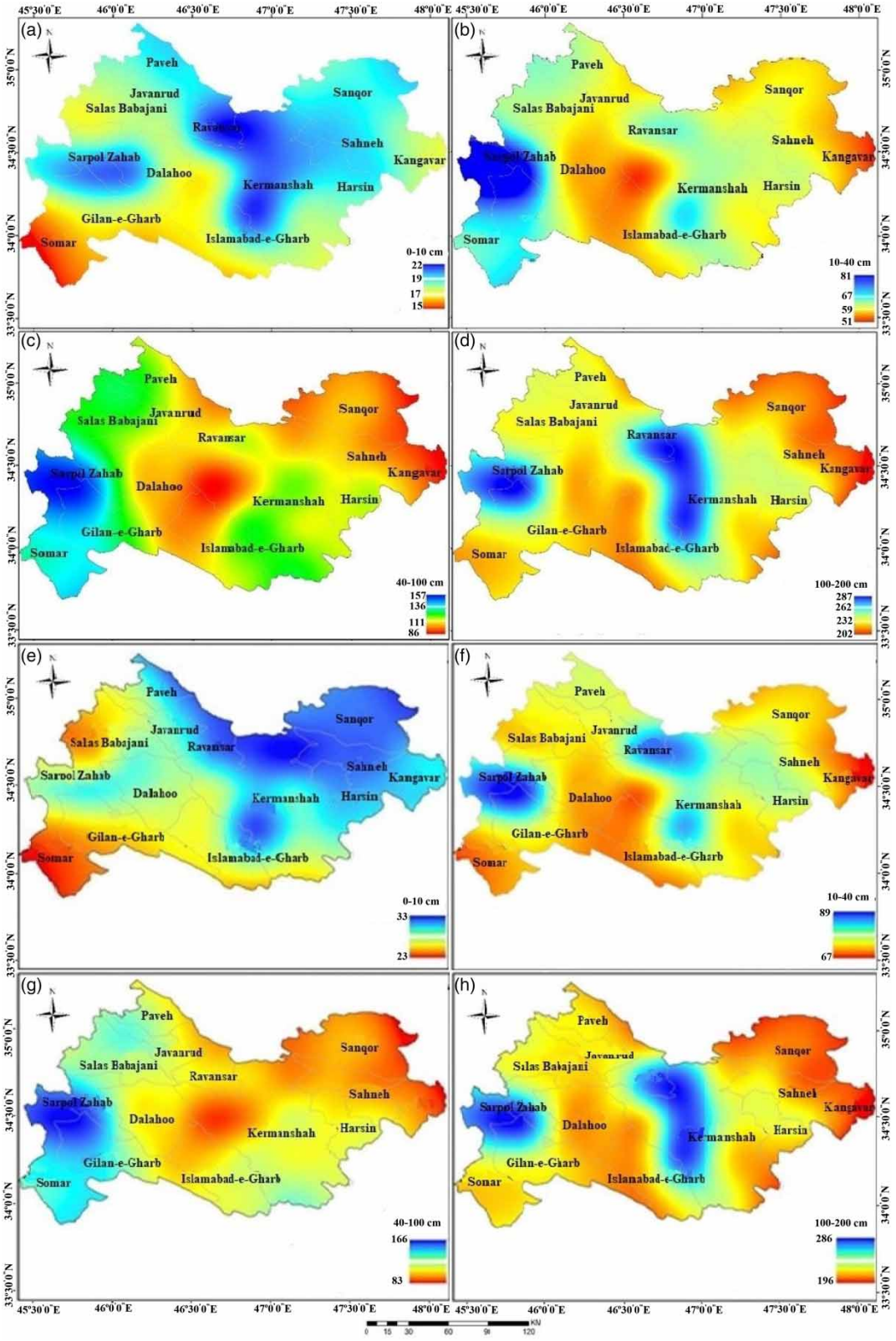

Figure 6 | Average soil moisture in the study area in (a) 0–10 cm; (b) 10–40 cm; (c) 40–100 cm; and (d) 100–200 cm and soil moisture situation in January during 2000–2014 based on GLDAS model in (e) 0–10 cm; (f) 10–40 cm; (g) 40–100 cm; and (h) 100–200 cm.

corresponds to the west, and the least was reported in the eastern portion of the area of study as reaching 86 kg/m^2 (Figure 6(c)). The soil moisture in this layer takes on similar conditions as in the 10–40 cm layer except that the areas of moisture loss in the 40–100 cm layer enjoy more spatial expansion, particularly in the

Downloaded from http://iwaponline.com/h2open/article-pdf/6/3/373/1255552/h2oj0060373.pdf
by guest

eastern part of the study area. The supreme moisture in soil average for the depth of 100–200 cm was reported to happen in Kermanshah city, Ravansar, and Sarpol Zahab as 287 kg/m^2, and the minimum turned out to be 202 kg/m^2 in Kangavar (Figure 6(d)). The minimum soil moisture cores were observed, for the depths 10–40 cm and 40–100 cm, in Kangavar and Sonqor, in the eastern part of the province. Scrutinizing the drought in Kermanshah province, Amini *et al.* (2019a, 2019b) concluded that the maximum occurrence of rainfall is in the north, and the minimum is in the southern parts. In the present research, the maxima and minima of the surface layer moisture are reported to happen in these areas as well. It seems that the climatic conditions have the most influence on the surface layer of the soil which is in the acceptable range with the results of Cai *et al.* (2017).

Zoning maps were supplied for various months. For instance, Figure 6(e)–6(h) portrays the soil moisture zoning for January. The maximum and minimum zones of soil moisture in this month in depth 0–10 cm were 33.18 and 22.63 kg/m^2, respectively. As for depths 10–40 cm, they are obtained as 89.08 and 66.71 kg/m^2, respectively, and for 40–100 cm the extremum values were 166.11 and 83.11 kg/m^2. Finally, for 100–200 cm, the highest and lowest extents of soil moisture were 286.09 and 195.72 kg/m^2, respectively. According to the zoning maps for all months, it is inferred that spatially for depths 0–10 cm the northern parts experience the maximum moisture of soil and the southern regions, especially south western areas, have the minimum moisture in nearly all months of the year. The maximum moisture cores for depths 10–40 cm disperse across the province so that Kermanshah city and Ravansar in the centre and north, and Sarpol Zahab in the west have the peak soil moisture. At these depths, the least moisture value belongs to Kangavar and Dalahoo. With regard to the depths of 40–100 cm, it could be mentioned that the dispersion of minimum moisture cores happened in the eastern and central portions of the research area, while the highest moisture is observed in Sarpol Zahab in the west. As to depths 100–200 cm, the dispersal of maximum moisture cores is typically in Kermanshah city and Ravansar in the centre, and in Sarpol Zahab in the western part of the province. Also, the lowest amount of moisture of soil arises in the east, south, and south-west of the province. In this latter depth, due to taking distance from the ground surface followed by the evaporation reduction, the soil moisture enjoys the least changes during the months of the year with almost similar situations of minimum and maximum cores throughout the year. By investigating the mapping of drought severity in Kermanshah province during the period under study and in the month of January, Amini *et al.* (2019a, 2019b) took the result that in January the most extreme drought concerns the south and south-west, and the least is associated with the north. This is in compliance with the soil moisture state in these areas. The studies conducted on the subject of the climatic conditions of the study area in the various statistical period show a positive correlation with the results of the current research (Moradi *et al.* 2016; Rajabi 2016; Bazrafshan 2017; Emadodin *et al.* 2019).

Drought and soil moisture

Table 3 shows some statistical properties for annual soil moisture and SPI at the depths of 100–200 cm from the ground.

The normalized soil moisture values and drought index SPI of the statistical period were computed using the annual precipitation values in the area under investigation. The pertaining results are inserted in Figure 7.

According to Figure 7, the minimum and maximum values of SPI are attained, respectively, in 2004 and 2009. This result shows that 2004 has been passed with the highest rainfall during the wet period and that the most severe drought has taken place in 2009. The greatest and least normalized soil moisture corresponded, respectively, to the very same years of 2004 and 2009. Hence, one deduces that the soil moisture values arising from GLDAS have a reverse relationship with the severity of drought and are in direct relation with SPI values, which agrees with the reported results by Sun *et al.* (2022). Moradi *et al.* (2016), Rajabi (2016), Bazrafshan (2017), and Emadodin *et al.* (2019) have shown, using the SPI values, that the area of Kermanshah has experienced extreme drought in the recent decade. This is in accordance with the annual soil moisture values given in the present research. Spennemann *et al.* (2015) showed that the moisture of soil values obtained from the

Table 3 | Statistical properties for annual soil moisture and SPI (100–200 cm)

Statistical properties	Average	Min.	Max.	Standard deviation	Coefficient of variation
Soil moisture	236.16	218.62	249.04	9.09	0.038
SPI	−0.123	−2.077	0.931	0.876	−7.09

Downloaded from http://iwaponline.com/h2open/article-pdf/6/3/373/1255552/h2oj0060373.pdf
by guest

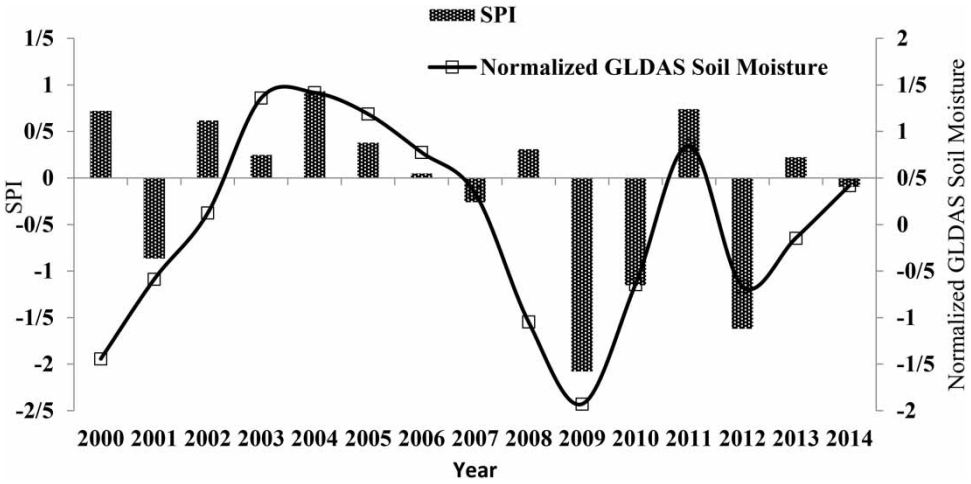

Figure 7 | Annually SPI and soil moisture values of the study area.

GLDAS model is in great correlation with those of SPI, in agreement with our results in the current work. Resorting to the moisture of soil in the monitoring of drought is an alternative adopted by several authors (Mo 2008; Houborg *et al.* 2012; Quan *et al.* 2012; Pozzi *et al.* 2013; Sedri *et al.* 2019).

CONCLUSION

In this research, we studied the spatial and temporal variations of soil moisture in Kermanshah province the GLDAS model. Statistical indicators were employed to evaluate the accuracy of moisture data given by GLDAS. Using these data, the monthly and annual soil moisture changes in depths 0–10, 10–40, 40–100, and 100–200 cm from the ground were inspected. The results taken via this investigation are as follows:

- The values of statistical indicators guaranteed that GLDAS data can be used with an acceptable approximation to estimate moisture in areas with limited or no data.
- The drought index, SPI, and soil moisture value were proven to be directly interrelated and hence, soil moisture had a reverse relation with drought severity.
- From data for various depths, it was found that the more severe the drought, the greater the effect on soil moisture in the deeper layers.
- The methodology used in this study can be adapted to monitor drought, fill the missing data of temporal and spatial series of soil moisture and overcome the problem of lack of soil moisture data in areas without synoptic stations.

FUNDING

This research received no external funding.

DATA AVAILABILITY STATEMENT

All relevant data are included in the paper or its Supplementary Information.

CONFLICT OF INTEREST

The authors declare there is no conflict.

REFERENCES

Aksoy, H., Cetin, M., Eris, E., Burgan, H. I., Cavus, Y., Yildirim, I. & Sivapalan, M. 2021 Critical drought intensity-duration-frequency curves based on total probability theorem-coupled frequency analysis. *Hydrological Sciences Journal* **66** (8), 1337–1358. 10.1080/02626667.2021.1934473.

Albergel, C., De Rosnay, P., Gruhier, C., Muñoz-Sabater, J., Hasenauer, S., Isaksen, L. & Wagner, W. 2012 Evaluation of remotely sensed and modelled soil moisture products using global ground-based *in situ* observations. *Remote Sensing of Environment* **118** (15), 215–226. https://doi.org/10.1016/j.rse.2011.11.017.

Downloaded from http://iwaponline.com/h2open/article-pdf/6/3/373/1255552/h2oj0060373.pdf
by guest

Alizamir, M., Heddam, S., Kim, S., Gorgij, A. D., Li, P., Ahmed, K. O. & Singh, V. P. 2021 Prediction of daily chlorophyll-a concentration in rivers by water quality parameters using an efficient data-driven model: online sequential extreme learning machine. *Acta Geophysica* **69** (1), 1–23.

Amini, A. 2020 The role of climate parameters variation in the intensification of dust phenomenon. *Natural Hazards* **102** (1), 445–468. doi:10.1007/s11069-020-03933-w.

Amini, A., Gharibreza, M., Shahmoradi, B. & Zareie, S. 2019a Land aptitude for horticultural crops and water requirement determination under unsustainable water resources condition. *Environmental Monitoring and Assessment* **191** (1), 1–13. doi:10.1007/s10661-018-7125-1.

Amini, A., Abdeh Kolahchi, A., Al-Ansari, N., Karami Moghadam, M. & Mohammad, T. 2019b Application of TRMM precipitation data to evaluate drought and its effects on water resources instability. *Applied Sciences* **9** (24), 5377. doi:10.3390/app9245377.

Bazrafshan, J. 2017 Effect of air temperature on historical trend of long-term droughts in different climates of Iran. *Water Resources Management* **31** (14), 4683–4698. doi:10.1007/s11269-017-1773-8.

Bi, H., Ma, J., Zheng, W. & Zeng, J. 2016 Comparison of soil moisture in GLDAS model simulations and *in situ* observations over the Tibetan Plateau. *Journal of Geophysical Research: Atmospheres* **121** (6), 2658–2678. doi:10.1002/2015JD024131.

Cai, J., Zhang, Y., Li, Y., Liang, X. S. & Jiang, T. 2017 Analyzing the characteristics of soil moisture using GLDAS data: a case study in eastern China. *Applied Sciences* **7** (6), 566. https://doi.org/10.3390/app7060566.

Chen, Y., Yang, K., Qin, J., Zhao, L., Tang, W. & Han, M. 2013 Evaluation of AMSR-E retrievals and GLDAS simulations against observations of a soil moisture network on the central Tibetan Plateau. *Journal of Geophysical Research: Atmospheres* **118** (10), 4466–4475. https://doi.org/10.1002/jgrd.50301.

Das, K. & Paul, P. K. 2015 Soil moisture retrieval model by using RISAT-1, C-band data in tropical dry and sub-humid zone of Bankura district of India. *The Egyptian Journal of Remote Sensing and Space Science* **18** (2), 297–310. https://doi.org/10.1016/j.ejrs.2015.09.004.

Das, N. N., Mohanty, B. P. & Njoku, E. G. 2008 A Markov chain Monte Carlo algorithm for upscaled soil-vegetation-atmosphere-transfer modeling to evaluate satellite-based soil moisture measurements. *Water Resources Research* **44** (5), W05416. https://doi.org/10.1029/2007WR006472.

Emadodin, I., Reinsch, T. & Taube, F. 2019 Drought and desertification in Iran. *Hydrology* **6** (3), 66. https://doi.org/10.3390/hydrology6030066.

Fang, L., Hain, C. R., Zhan, X. & Anderson, M. C. 2016 An inter-comparison of soil moisture data products from satellite remote sensing and a land surface model. *International Journal of Applied Earth Observation and Geoinformation* **48**, 37–50. https://doi.org/10.1016/j.jag.2015.10.006.

FAO. 2015 *World Reference Base for Soil Resources 2014, Update 2015, World Soil Resources Reports No. 106*. FAO, Rome. Available from: http://www.fao.org/3/i3794en/I3794en.pdf.

Fatemi, M. & Narangifard, M. 2018 Study of spatial and temporal rain and drought patterns in the south of Iran using TRMM. *Desert* **23** (2), 243–253. Available from: https://jdesert.ut.ac.ir/article_69121_8791.html.

Houborg, R., Rodell, M., Li, B., Reichle, R. & Zaitchik, B. F. 2012 Drought indicators based on model-assimilated Gravity Recovery and Climate Experiment (GRACE) terrestrial water storage observations. *Water Resources Research* **48** (7), W07525. https://doi.org/10.1029/2011WR011291.

Ji, L. & Gallo, K. 2006 An agreement coefficient for image comparison. *Photogrammetric Engineering & Remote Sensing* **72** (7), 823–833.

Kim, H. & Choi, M. 2015 Impact of soil moisture on dust outbreaks in East Asia: using satellite and assimilation data. *Geophysical Research Letters* **42** (8), 2789–2796. https://doi.org/10.1002/2015GL063325.

Lakhankar, T., Jones, A. S., Combs, C. L., Sengupta, M., Vonder Haar, T. H. & Khanbilvardi, R. 2010 Analysis of large scale spatial variability of soil moisture using a geostatistical method. *Sensors* **10**, 913–932. https://doi.org/10.3390/s100100913.

Li, D., Zhao, T., Shi, J., Bindlish, R., Jackson, T. J., Peng, B. & Han, B. 2015 First evaluation of Aquarius soil moisture products using in situ observations and GLDAS model simulations. *IEEE Journal of Selected Topics in Applied Earth Observations and Remote Sensing* **8** (12), 5511–5525. doi:10.1109/JSTARS.2015.2452955.

Liu, Y., Liu, Y. & Wang, W. 2019 Inter-comparison of satellite-retrieved and global land data assimilation system-simulated soil moisture datasets for global drought analysis. *Remote Sensing of Environment* **220** (2019), 1–18. https://doi.org/10.1016/j.rse.2018.10.026.

Mo, K. C. 2008 Model-based drought indices over the United States. *Journal of Hydrometeorology* **9** (6), 1212–1230. https://doi.org/10.1175/2008JHM1002.1.

Moradi, M., Yahya Safari, S., Biglari, H., Ghayebzadeh, M. & Darvishmotevalli, M. 2016 Multi-year assessment of drought changes in the Kermanshah city by standardized precipitation index. *International Journal of Pharmacy & Technology* **8**, 17975–17987. Available from: http://eprints.gmu.ac.ir/id/eprint/64.

Ouatiki, H., Boudhar, A., Tramblay, Y., Jarlan, L., Benabdelouhab, T., Hanich, L., Chehbouni, A., El Meslouhi, M. R. & Chehbouni, A. 2017 Evaluation of TRMM 3b42 V7 rainfall product over the Oum Er Rbia watershed in Morocco. *Climate* **5** (1), 1–17. https://doi.org/10.3390/cli5010001.

Park, S., Park, S., Im, J., Rhee, J., Shin, J. & Park, J. D. 2017 Downscaling GLDAS soil moisture data in East Asia through fusion of multi-sensors by optimizing modified regression trees. *Water* **9** (5), 332. https://doi.org/10.3390/w9050332.

Downloaded from http://iwaponline.com/h2open/article-pdf/6/3/373/1255552/h2oj0060373.pdf
by guest

Pozzi, W., Sheffield, J., Stefanski, R., Cripe, D., Pulwarty, R., Vogt, J. V., Heim, R. R., Brewer, M. J., Svoboda, M., Westerhoff, R., van Dijk, A. I. J. M., Lloyd-Hughes, B., Pappenberger, F., Werner, M., Dutra, E., Wetterhall, F., Wagner, W., Schubert, S., Mo, K., Nicholson, M., Bettio, L., Nunez, L., van Beek, R., Bierkens, M., Goncalves, L. G. G. de, Mattos, J. G. Z. & Lawford, R. 2013 Toward global drought early warning capability: expanding international cooperation for the development of a framework for monitoring and forecasting. *Bulletin of the American Meteorological Society* **94** (6), 776–785. https://doi.org/10.1175/BAMS-D-11-00176.1.

Quan, X. W., Hoerling, M. P., Lyon, B., Kumar, A., Bell, M. A., Tippett, M. K. & Wang, H. 2012 Prospects for dynamical prediction of meteorological drought. *Journal of Applied Meteorology and Climatology* **51** (7), 1238–1252. https://doi.org/10.1175/JAMC-D-11-0194.1.

Rajabi, A. 2016 Analysis of SPI drought class transitions due to climate change. case study: Kermanshah (Iran). *Water Resources* **43** (1), 238–248. doi:10.1134/S0097807816120010.

Rodell, M., Houser, P. R., Jambor, U. E. A., Gottschalck, J., Mitchell, K., Meng, C. J., Arsenault, K., Cosgrove, B., Radakovich, J., Bosilovich, M., Entin, J. K., Walker, J. P., Lohmann, D. & Toll, D. 2004 The global land data assimilation system. *Bulletin of the American Meteorological Society* **85** (3), 381–394. https://doi.org/10.1175/BAMS-85-3-381.

Sedri, M. H., Amini, A. & Golchin, A. 2019 Evaluation of nitrogen effects on yield and drought tolerance of rainfed wheat using drought stress indices. *Journal of Crop Science and Biotechnology* **22** (3), 235–242. https://doi.org/10.1007/s12892-018-0037-0.

Shen, Q., Lin, J., Yang, J., Zhao, W. & Wu, J. 2022 Exploring the potential of spatially downscaled solar-induced chlorophyll fluorescence to monitor drought effects on gross primary production in winter wheat. *IEEE Journal of Selected Topics in Applied Earth Observations and Remote Sensing* **15**, 2012–2022. doi:10.1109/JSTARS.2022.3148393.

Skierucha, W., Wilczek, A., Szypłowska, A., Sławiński, C. & Lamorski, K. 2012 A TDR-based soil moisture monitoring system with simultaneous measurement of soil temperature and electrical conductivity. *Sensors* **12** (10), 13545–13566. https://doi.org/10.3390/s121013545.

Spennemann, P. C., Rivera, J. A., Saulo, A. C. & Penalba, O. C. 2015 A comparison of GLDAS soil moisture anomalies against standardized precipitation index and multisatellite estimations over South America. *Journal of Hydrometeorology* **16** (1), 158–171. https://doi.org/10.1175/JHM-D-13-0190.1.

Sun, P., Ma, Z., Zhang, Q., Singh, V. P. & Xu, C. Y. 2022 Modified drought severity index: model improvement and its application in drought monitoring in China. *Journal of Hydrology* **612**, 128097. https://doi.org/10.1016/j.jhydrol.2022.128097.

Um, M. J., Kim, Y. & Park, D. 2018 Evaluation and modification of the drought severity index (DSI) in East Asia. *Remote Sensing of Environment* **209**, 66–76. https://doi.org/10.1016/j.rse.2018.02.044.

Velde, R., Salama, M. S., Pellarin, T., Ofwono, M., Ma, Y. & Su, Z. 2014 Long term soil moisture mapping over the Tibetan plateau using special sensor microwave/imager. *Hydrology and Earth System Sciences* **18** (4), 1323–1337. https://doi.org/10.5194/hess-18-1323-2014.

Wagner, W., Scipal, K., Pathe, C., Gerten, D., Lucht, W. & Rudolf, B. 2003 Evaluation of the agreement between the first global remotely sensed soil moisture data with model and precipitation data. *Journal of Geophysical Research: Atmospheres* **108** (D19). https://doi.org/10.1029/2003JD003663.

Wagner, W., Dorigo, W., de Jeu, R., Fernandez, D., Benveniste, J., Haas, E. & Ertl, M. 2012 Fusion of active and passive microwave observations to create an essential climate variable data record on soil moisture. *ISPRS Annals of the Photogrammetry, Remote Sensing and Spatial Information Sciences (ISPRS Annals)* **7**, 315–321.

Xiao, Z., Jiang, L., Zhu, Z., Wang, J. & Du, J. 2016 Spatially and temporally complete satellite soil moisture data based on a data assimilation method. *Remote Sensing* **8** (1), 49. https://doi.org/10.3390/rs8010049.

Yan, N., Wu, B., Chang, S. & Bao, X. 2014 Evaluation of TRMM precipitation product for meteorological drought monitoring in Hai Basin. In *IOP Conference Series: Earth and Environmental Science*. (Vol. 17, No. 1, p. 012093). IOP Publishing. doi:10.1088/1755-1315/17/1/012093.

Yuan, S. & Quiring, S. M. 2017 Evaluation of soil moisture in CMIP5 simulations over the contiguous United States using in situ and satellite observations. *Hydrology and Earth System Sciences* **21** (4), 2203–2218. doi:10.5194/hess-21-2203-2017.

Zeng, Y., Su, Z., Van der Velde, R., Wang, L., Xu, K., Wang, X. & Wen, J. 2016 Blending satellite observed, model simulated, and in situ measured soil moisture over Tibetan Plateau. *Remote Sensing* **8** (3), 268. https://doi.org/10.3390/rs8030268.

Zhang, Q., Xiao, F., Niu, H. & Dong, W. 2005 Analysis of vegetation index sensitivity to soil moisture in Northern China. *Chinese Journal of Ecology* **24** (7), 715–718.

Zhuang, R., Zeng, Y., Manfreda, S. & Su, Z. 2020 Quantifying long-term land surface and root zone soil moisture over Tibetan Plateau. *Remote Sensing* **12** (3), 509. https://doi.org/10.3390/rs12030509.

Zuo, J., Xu, J., Li, W. & Yang, D. 2019 Understanding shallow soil moisture variation in the data-scarce area and its relationship with climate change by GLDAS data. *Plos One* **14** (5), e0217020. https://doi.org/10.1371/journal.pone.0217020.

First received 4 April 2023; accepted in revised form 24 June 2023. Available online 7 July 2023

Downloaded from http://iwaponline.com/h2open/article-pdf/6/3/373/1255552/h2oj0060373.pdf
by guest